SciMedCentral

JSM Nanotechnology & Nanomedicine

Review Article

Dielectrophoresis of Biomolecules

David J. Bakewell[1], Nuria Vergara-Irigaray[2] and David Holmes[3]*

[1]*Department of Electrical Engineering and Electronics, University of Liverpool, L69 3GJ, UK*

[2]*Department of Genetics, Evolution and Environment, Institute of Healthy Ageing, University College London, Gower Street, London WC1E 6BT, UK*

[3]*London Centre for Nanotechnology, University College London, 17-19 Gordon Street, London, WC1H 0AH, UK*

Corresponding author

Dr. David Holmes, London Centre for Nanotechnology, University College London, 17-19 Gordon Street, London, WC1H 0AH, UK, Email: david.holmes@ucl.ac.uk

Submitted: 31 July 2013

Accepted: 05 August 2013

Published: 07 August 2013

Keywords

- Dielectrophoresis
- Biomolecules
- DNA
- RNA
- Polarizability
- Dielectrophoretic spectroscopy
- AC Electrokinetics
- Nanoparticle characterization

Abstract

Principles and applications of dielectrophoresis (DEP) of biomolecules, suspended in aqueous medium, are reviewed. Biomolecules include nucleic acids (DNA and RNA), proteins, carbohydrates and lipids, and vary significantly in their composition and their behavior in aqueous medium. Review of dielectric polarisability principles and DEP fundamentals, therefore, focuses on two important biomolecules of interest in today's laboratory: double stranded DNA and ideal biocolloids (nanospheres). These examples demonstrate two key mechanisms of inducible polarisability that gives rise to DEP motion: Maxwell-Wagner (MW) interfacial polarization and counterion polarization. DNA behaves as a worm-like chain in aqueous suspension with an often poorly defined biomolecule-solution interface, and DEP motion is induced mainly by counterion response to oscillating electric fields. On the other hand, nanospheres, with their well-defined particle-solution interface, tend to involve mainly MW polarization in their DEP-driven motion. DEP of DNA and RNA often involves manipulation in conjunction with nanospheres and other nanoscale surfaces, such as, the probe tips of scanning microscopes. The review closes with future outlook and opportunities for further investigation using emerging technologies and automation methods.

INTRODUCTION

Dielectrophoresis (DEP) is the translational motion of an electrically polarisable body by the action of an externally applied, spatially non-uniform, electric field. DEP can occur with an electrically neutral body in a spatially non-uniform field and depends on the dielectric properties of the body relative to the surrounding medium [1,2]. The word *dielectrophoresis* is the conjunction of two parts: *dielectro* – referring to the dependence of the motion on the dielectric properties of the body, and *phoresis* – referring to motion. DEP is distinguished from *electrophoresis* that requires a net charge on the body for Coulombic movement to occur in an externally applied, spatially uniform, electric field. This means that DEP can be used to move and manipulate very small biomolecules, whether or not they carry a net electrical charge. DEP is also independent of the direction of the electric field so that AC voltages, at sufficient radio frequencies (RFs) that avoid problematic hydrolysis at the solution-electrode interface, can be used to induce DEP-driven motion. These properties make DEP a very popular and a relatively cheap method of controlling biomolecular movement, particularly using low voltages in a micro-device environment, such as, Lab-On-Chip (LOC) or micro-Total Analysis System (μTAS) application. DEP is also distinguished from electrorotation (ROT) that refers to *rotational* motion of a body in a spatially inhomogeneous electric field.

Biomolecules are organic molecules that are biologically important and include nucleic acids, proteins, carbohydrates and lipids [3]. The nucleic acids are deoxyribonucleic acid (DNA), ribonucleic acid (RNA), and synthetically made polynucleic acid (PNA). This article focuses on nucleic acids, DNA and RNA, leaving proteins, carbohydrates and lipids for another review. Included in the discussion, are bio-colloidal nanospheres, that are often functionalized with biomolecules and are powerful tools in today's laboratory. The article reviews the basic theoretical principles of dielectric polarization that lead to DEP motion, and then describes interesting applications of DEP of DNA and RNA, in combination with nanospheres. Theoretical principles, for convenience, are focused on two biomolecules that are prominent in the DEP literature, and serve as important examples: DNA that behaves as a stringy, worm-like chain in water, and nanospheres that behave very differently to DNA - as ideal bio-colloids, or compact biomolecules - with well-defined particle-solution interface.

PROPERTIES OF BIOMOLECULES AND PRINCIPLES OF DIELECTROPHORESIS

Understanding the motion of biomolecules suspended

in aqueous solution, to an externally applied electrical field, depends on a number of factors including the electrical charge of the constituent chemical groups and the ionic charges in the suspending medium.

Electrical and mechanical properties of biomolecules

Biological polyelectrolytes are molecules with a large number of charged chemical groups, and examples include DNA and collagen. Biomolecules, such as, DNA and RNA possess a net *negative* charge. An electrolyte or aqueous environment with salts acts as a supply for dissociated ions for example, Na^+, Mg^{2+}, OH^-, Cl^-. Consequently, if the biomolecule is electrically charged, it will attract ions of the opposite charge (or *counterions*) by Coulombic forces in order to restore charge neutrality. These counterions form a cloud around the biomolecule and act to electrically screen in the biomolecule by a certain amount. Further away from the biomolecule, the charge of the counterions themselves, in turn, attracts ions of the opposite charge that have the same charge as the biomolecule and are termed *co-ions*.

Electrical double layer

Investigations on the behavior of biological polyelectrolytes and biocolloids have indicated the presence of an electrical double layer, shown in (Figure 1). Counterions adjacent and close to the biomolecule form the Stern layer. Counterions further away from the biomolecule and Stern layer are more diffuse and screen the biomolecule charge in such a way as to attract co-ions. This diffuse layer has characteristic length, λ_D, as shown and is referred to as the Debye screening length. In conjunction with the Coulombic and diffusive forces, the diffuse layer is subjected to hydrodynamic forces. The 'slip plane' designates where the part of the diffuse layer that moves with the body, relative to the remainder that tends to be dragged away by the surrounding medium. The zeta potential Φ_ζ (not shown in Figure 1) is the electrical potential at the slip plane [4,5].

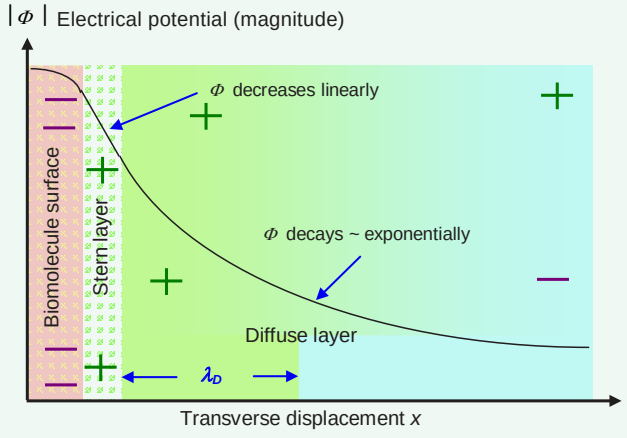

Figure 1 Electric double layer schematic representation. The electrical double-layer scheme surrounding a biomolecule surface with potential magnitude Φ superposed: a layer of negative charges at the biomolecule surface is surrounded by a positively charged counterion layer. This consists of a thin Stern layer and diffuse layer with characteristic length, λ_D (not to scale).

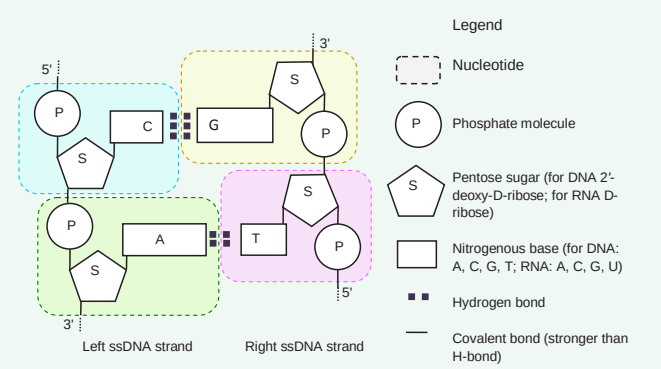

Figure 2 Building blocks of dsDNA schematic representation. Ladder sketch of dsDNA showing the constituents of each nucleotide containing a base, sugar (S), and phosphate (P), and pairing of left and right strands. Not to scale; for twist and writhe angles between molecules in 3D, see text for references.

Chemical and biological properties of DNA

The basic building blocks of DNA are nucleotides shown in (Figure 2). Each nucleotide consists of a nitrogenous base that is one of four possibilities: either a purine - Adenine (A) or Guanine (G), or pyrimidine - Cytosine (C) or Thymine (T). In addition to the base, is a pentose sugar ring (2' – deoxy-D-ribose, denoted 'S') and a phosphate molecule ,'P'. The spatial arrangement of the three constituents for each the four nucleotides that comprise DNA are shown in the figure**.** The nucleotides are covalently linked together with the phosphates acting as bridges between the pentose sugars. The 5´ - phosphate group of one nucleotide is linked to the 3´ - hydroxyl group of the next nucleotide. The linkages are often referred to as the 'sugar phosphate backbone'.

DNA can exist as either double stranded (dsDNA) or single stranded (ssDNA). A key property of DNA is that a single strand of linked nucleotides can form complementary pairs with another strand. That is, each base of a nucleotide on one strand can form hydrogen (H) bonds with the base of a nucleotide on the opposite strand. This occurs for all bases on each strand with purines pairing with pyrimidines. Figure 2 shows base pairing where A and C on the left strand forms H-bonds with T and G on the right strand. There are different forms of dsDNA, namely A, B, and Z [6]. The standard double helical DNA usually referred to is (Crick and Watson) B-form.

Figure 3 shows a very short length of dsDNA as it occurs in aqueous (or water) solution, that is, in the energetically favourable state as a double helix. The sugar-phosphate double helical backbones are shown as thick lines with bases pairing as A with T, and G with C. Structurally 'backbone' is somewhat misleading as it is the stacking of the nitrogen bases that gives the molecule its mechanical stiffness [6]. The sugar-phosphate backbones confer negative charge to DNA and being hydrophilic they lie on the exterior of the biomolecule. The hydrophobic nucleotide base-pairs (bp) lie within the biomolecule, away from the polar water molecules. They are represented symbolically (A – T, C – G pairs) with respective double and triple H-bonds. The displacement along the major helical axis between base pairs is shown as 0.34 nm, so that the length between repetitive positions

of the double helix is about 3.6 nm (10.5 bp). The diameter is about 2 nm.

Importantly, the H-bonds shown in (Figures 2 and 3), are weaker than the covalent bonds. This means that by moderate heating, or by using a different solvent, each dsDNA biomolecule can be reversibly separated into two complementary ssDNA strands. These ssDNA strands, in a solution with available nucleotides bases, can act as templates, thus enabling *replication*. They also enable detection: a ssDNA with a particular sequence will pair up with another ssDNA with the complementary sequence. In situations where a particular base does not match (e.g. A – A**)** and the others do, it is called a *mismatch*. These fundamental properties underpin the emergence of new technologies, such as, nanospheres and microarrays, where applications of DEP are being explored for enhancing concentration and other developments – as described as described later in this review article.

In (Figure 3) dsDNA is shown as straight but this feature only applies for relatively short lengths. The mechanical properties of dsDNA are partly determined by the stacking of the nitrogen bases of dsDNA, and ssDNA is comparatively much more flexible. The flexibility of DNA also depends on the ionic composition of the solvent. In the situation of low concentration of counterions there is little electrostatic screening of the polyelectrolyte with itself. That is, the biomolecule electrostatically repels itself, so to be energetically favorable it tends to be straight. Conversely,

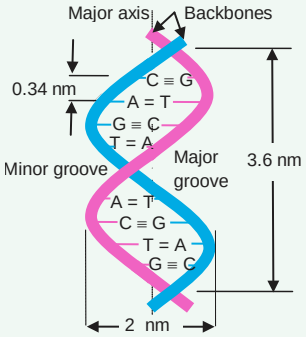

Figure 3 Double helical dsDNA schematic representation. A short fragment of dsDNA as it appears in aqueous solution, double helical B-form. See text for details.

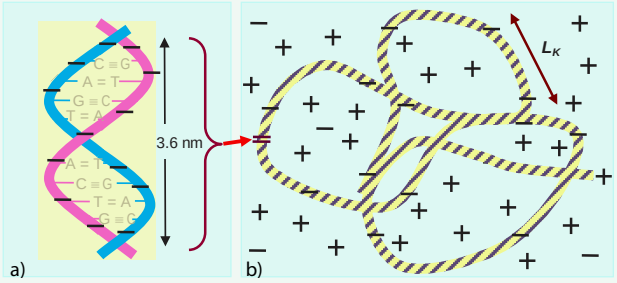

Figure 4 (a) dsDNA and (b) worm-like DNA. dsDNA (or DNA) as a negatively charged polyelectrolyte in solution attracts counterions (mostly cations). These form around the polyelectrolyte to electrostatically screen the charge of the DNA. Worm-like chain model of dsDNA,with close-up inset, in aqueous suspension, showing relatively straight segments of Kuhn length L_K. Not to scale.

in solvents with high molar counterion concentrations, screening occurs to the extent the biomolecule repels itself less, so it is more flexible.

DNA can be modeled as a worm-like chain

A measure of straightness is known as the persistence length, L_p, as sketched in (Figure 4). Typically for standard biological conditions for dsDNA, L_p = 50 nm [7]. The behavior of dsDNA in water is modeled as a worm-like chain with each straight link equal to the Kuhn length that is twice the persistence length, $L_K = 2L_p$ [8]. In this chain, due to thermal motion, the next link is independently and randomly oriented from the previous link. Each link is about 100 nm or about 300 bp. The persistence length of ssDNA is much shorter than dsDNA, about 1 nm. The following discussion on dielectric polarization mechanisms includes both DNA and RNA but focuses on DNA since the literature, reviewed in [7], is much more extensive. In addition, dielectric spectroscopic measurements of the electrical properties of ribosomal RNA are often confounded by the presence of ribosomal proteins [9].

A biomolecule moving in a solvent (e.g. DNA in water) can behave hydrodynamically as if it is a rigid body, such as, a sphere. This is due to the worm-like chain retaining a roughly spherical (or ellipsoidal) shape due to ions and water molecules being attracted and dragged along with it. The mass of DNA, ions and water exerts a hydrodynamic drag equivalent to a sphere with a radius, r_h. This is the hydrodynamic radius and is an important parameter that can be estimated from experimental measurements [8].

Dielectric polarization

Dielectric polarization describes how charges, within a dielectric, respond to an externally applied electric field. Charges that are free to move over a long range reveal their movement on a macroscopic scale as conduction. If the movement of the charges is restricted they are said to be 'polarised' [1]. In this respect, polarisation is the 'capability' of the charges to move in response to an applied electric field. The polarisation can be expressed, in terms of an equivalent circuit with permittivity parameters, as the real (in-phase) permittivity ε' or *dielectric constant* and the free movement of charges as the imaginary (out-of phase) permittivity ε'', or *dielectric loss*. The permittivity parameters are frequency dependent, $\varepsilon \equiv \varepsilon(\omega)$. In addition, the conductivity (or low frequency Ohmic loss) of the electrolyte solution, σ is included [4,10-12]. The complex permittivity ε is the combination of these,

$$\varepsilon(\omega) = \varepsilon'(\omega) - j[\varepsilon''(\omega) + \sigma / \omega] \quad (1)$$

where $j = \sqrt{-1}$, the angular frequency is $\omega = 2\pi f$ (rad s^{-1}) with frequency f (Hz). Often $\varepsilon'' << \sigma / \omega$, the superscript $'$ notation is omitted in the literature and the complex permittivity is written

$$\underline{\varepsilon}^* = \varepsilon - j\sigma / \omega \quad (2)$$

where the underscore denotes a complex quantity, '*' denotes conjugate and ε is the permittivity (real part of $\underline{\varepsilon}^*$) that is assumed constant for the frequencies of interest.

A quantitative measure of the responsiveness of a body to

an applied external electric field, is the polarisability, α. A highly polarisable body, for example, features many charges that are responsive to an electric field and their movement is in some way restricted. An important parameter for experimentally determining the value of the polarizability of a biomolecule, such as, DNA, is the dielectric increment, or decrement [10,12],

$$\Delta\varepsilon' = \varepsilon'_{rl} - \varepsilon'_{rh} \tag{3}$$

where ε'_{rl} and ε'_{rh} are the low and high frequency relative permittivities, or limiting dielectric constants. The predicted polarizability α_m for a biomolecule determined using the experimentally measured dielectric decrement $\Delta\varepsilon'$ is given by

$$\alpha_m = \frac{3\varepsilon_o \Delta\varepsilon'}{C_m} \tag{4}$$

where ε_0 is the permittivity of free space, C_m is the number density (m^{-3}) of biomolecules and the factor '3' accounts for random biomolecular orientation. Using dielectric mixture theory, the polarizability of each DNA or RNA biomolecule can be determined from the suspension by calculating the volume fraction of the biomolecule. Another parameter is the relaxation time constant, τ_R (s) that is the time duration for charges to redistribute, or 'relax' after being perturbed by an electric field. The charges resonate at a dispersion frequency, f_R, or angular frequency ω_R,

$$\tau_R = \frac{1}{f_R} = \frac{2\pi}{\omega_R} \tag{5}$$

Dispersions arise when the oscillating cloud of charges can no longer follow the alternating electric field and this effect is observed in both real and imaginary parts of the complex permittivity. Biomolecules often have more than one dielectric dispersion characterized by a decrement and associated time constant. Commercial time-domain dielectric spectrometers can be used to estimate the dispersion decrement $\Delta\varepsilon'$ and time constant τ_R using a sample, e.g. 150 microlitres (μl), of biomolecules suspended in a solvent, such as, water. Characteristics of dielectric permittivities and losses for calf-thymus DNA, a biomolecule used in many dielectric spectroscopy studies, versus frequency are compiled and shown in [7]. Although there are variations in the experimentally measured permittivity ε', they all tend to decrease with increase in frequency and the polarisability follows the same trend.

The types of polarisation include electronic, atomic, molecular, interfacial (or space-charge), and counterion polarisation. The first three are attributed to the displacement, or orientation, of bound charges; the latter two concern movement on a larger scale. Of the first three types of polarisation, only molecular dipole polarisation, tends to feature in the literature concerning dielectric properties of biomolecules. The asymmetric distribution of electrons in molecules gives rise to *permanent* dipoles. The interaction of such a dipole with an externally applied electric field causes a torque that attempts to orient the molecule in the field direction. The polarisation is appropriately called *orientation*, or *dipole*, polarisation. Water is an example of a molecule with a permanent dipole and manifests permittivity values, via ε and σ, that are practically frequency independent up to 17 GHz [11].

The last two kinds of polarisation, interfacial and counterion, involve large-scale charge movement. Currently, there is no universal consensus in the literature on the high frequency polarisation mechanisms for biomolecules, such as, DNA or RNA. At present, the emphasis tends to favour Maxwell-Wagner interfacial polarisation for molecular structures with well-defined interfaces with water molecules, and counterion fluctuation polarisation, along the longitudinal axis, for DNA and similarly for RNA.

Maxwell-Wagner interfacial polarization

A schematic diagram of Maxwell-Wagner (MW) interfacial polarisation for an electrically neutral bio-colloid (nano-sphere) suspended in aqueous solution is shown in (Figure 5). The biomolecule lies in a uniform electric field established by an electric potential difference being applied between two parallel plates. The charges have moved to their interfaces in accordance with Coulomb's law and their movement is the same throughout the bio-colloid. Consequently, the interaction of the uniform external field with the charges means the sum of the forces is zero and the neutral body does not move.

If the potential on the electrodes is suddenly reversed to that they are opposite to the values shown in (Figure 5), then, there will be a time delay before the charges redistribute themselves, inside the body, to the imposed electric field. There will also be a delay for the counterions to re-cluster around the polarised body. The time taken for the charges to redistribute, or 'relax', is called the *relaxation time*. The movement of the charges, restricted by interfaces between layers, manifests itself as polarisation. The delay also occurs when the electrode potentials are reversed, again, back to the original state. Thus, applying an AC electric potential across the electrodes causes the charges within the bio-colloid to attempt to respond to temporal changes in the electric field.

There have been a number of investigations on polarisation mechanisms of colloids and polyelectrolytes with spherical geometry, [13-19]. The expression for the effective polarisability,

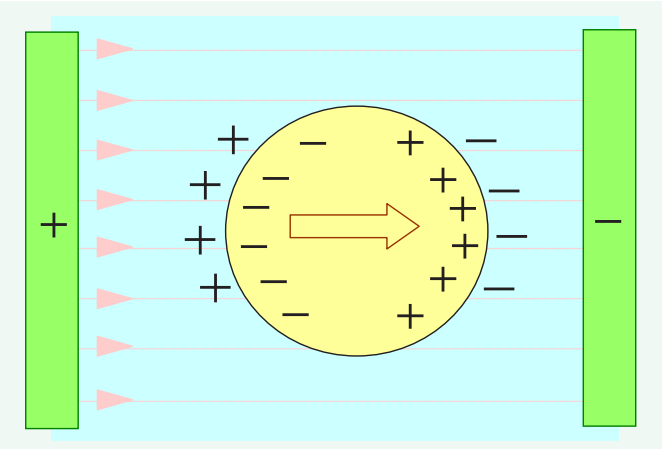

Figure 5 MW polarization for neutral sphere. Maxwell-Wagner (MW) interfacial polarisation of a neutral dielectric body, such as an ideal bio-colloid, in a uniform field. Charges accumulate at the interface between the dielectric sphere and the aqueous medium.

α, or dipole moment per unit volume per unit electric field, for interfacial polarisation of a spherical particle immersed in a medium is [20,21],

$$\alpha = 3\varepsilon_m \,\mathrm{Re}\{f_{CM}(\omega)\} = 3\varepsilon_m \,\mathrm{Re}\left\{\frac{\underline{\varepsilon}_p^* - \underline{\varepsilon}_m^*}{\underline{\varepsilon}_p^* + 2\underline{\varepsilon}_m^*}\right\} \quad (6)$$

where $\underline{\varepsilon}_p^* = \varepsilon_p - j\sigma_p/\omega$ is the complex permittivity of the particle, $\underline{\varepsilon}_m^* = \varepsilon_m - j\sigma_m/\omega$ is the complex permittivity of the medium,' Re{...} ' denotes the real part of the frequency dependent Clausius-Mossotti function, f_{CM}. It is assumed the particle lies in a homogenous external electric field, shown in (Figure 5), and the permittivity and conductivity parameters, ε and σ, are implicitly assumed to be frequency independent. Substituting the relations for the complex permittivities,

$$\mathrm{Re}\{f_{CM}(\omega)\} = \left[\frac{(\sigma_p - \sigma_m)(\sigma_p + 2\sigma_m) + \omega^2(\varepsilon_p - \varepsilon_m)(\varepsilon_p + 2\varepsilon_m)}{(\sigma_p + 2\sigma_m)^2 + \omega^2(\varepsilon_p + 2\varepsilon_m)^2}\right] \quad (7)$$

By considering the two conditions $\sigma_p >> \sigma_m$, $\sigma_p << \sigma_m$ for the limiting case $\omega \to 0$, and $\varepsilon_p >> \varepsilon_m$, $\varepsilon_p << \varepsilon_m$ for $\omega \to \infty$, it is evident, $-0.5 \le \mathrm{Re}\{f_{CM}(\omega)\} \le 1$.

An example plot of the real part of the Clausius-Mossotti function for a 216 nm diameter nanosphere is shown in (Figure 6) for $10^3 \le f \le 10^9$ Hz with $\varepsilon_m = 78.4\varepsilon_0$ and $\varepsilon_p = 2.55\varepsilon_0$ [22] where the permittivity of free space is $\varepsilon_0 = 8.854\times10^{-12}$ F/m, r = 108 nm, σ_m = 1.7 mS/m. The conductivity of the particle (bead) σ_p, of radius r, consists of the bulk conductivity σ_b of the body and a contribution from ion movement shunted around, tangential, to the surface of the particle [13] with surface conductance, K_s (S). K_s includes ion movement in both parts of the double layer described earlier [23],

$$\sigma_p = \sigma_b + 2K_s/r \quad (8).$$

Substituting typical values, σ_b = 0 and K_s = 1.0 nS, then σ_p = 18.5 mS/m. In (Figure 6) an important transition occurs at $\mathrm{Re}\{f_{CM}(\omega)\} = 0$ and is called the *cross-over frequency*. In the following section, it is shown that the DEP force is proportional to the polarisability, $\vec{F}_{DEP} \propto \alpha$, so that positive DEP (pDEP) occurs when $\mathrm{Re}\{f_{CM}(\omega)\} > 0$ and the particle moves towards the region of maximum variation in the electric field intensity. Conversely, negative DEP occurs when $\mathrm{Re}\{f_{CM}(\omega)\} < 0$, and the direction of the force is towards electric field minima. The conditions for positive and negative DEP also apply to non-spherical geometry [21]. Applying the condition $\mathrm{Re}\{f_{CM}\} = 0$ in (7), establishes the relationship between cross-over frequency $f = f_c$ and medium conductivity for these bio-colloids,

$$f_c = \frac{1}{2\pi}\sqrt{\frac{(\sigma_p - \sigma_m)(\sigma_p + 2\sigma_m)}{(\varepsilon_m - \varepsilon_p)(\varepsilon_p + 2\varepsilon_m)}} \quad (9)$$

The cross-over frequency is shown in (Figure 6) to be slightly above 3 MHz. Analysis of the transient response of the sphere to an electric field reveals a MW relaxation time constant τ_{MW} associated with free charge storage at the spherical interface [21]

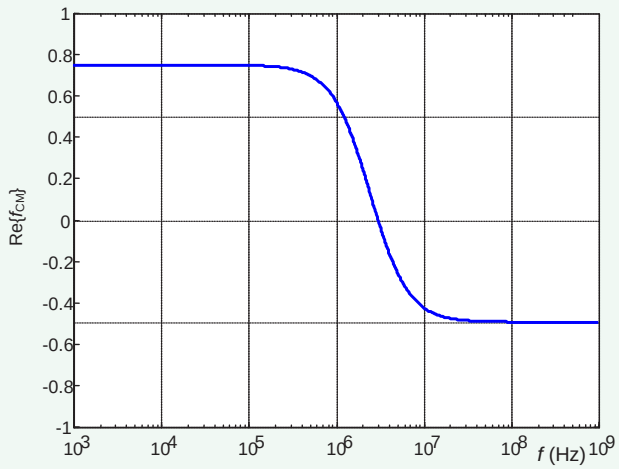

Figure 6 Real part of CM. Plot of the real part of the frequency dependent Clausius-Mossotti function, Re{f_{CM}}. The plot crosses-over from positive to negative at about 3 MHz.

$$\tau_{MW} = \frac{\varepsilon_p + 2\varepsilon_m}{\sigma_p + 2\sigma_m} \quad (10).$$

The relaxation time constant enables (7) to be re-cast [21,24],

$$\mathrm{Re}\{f_{CM}(\omega)\} = \left[\frac{\varepsilon_p - \varepsilon_m}{\varepsilon_p + 2\varepsilon_m} + \frac{3(\varepsilon_m\sigma_p - \varepsilon_p\sigma_m)}{\tau_{MW}(\sigma_p + 2\sigma_m)^2(1 + \omega^2\tau_{MW}^2)}\right] \quad (11)$$

and reveals that the conductivity parameters dominate at low frequencies, and the permittivities at high frequencies,

$$\mathrm{Re}\{f_{CM}(\omega)\} = \begin{cases} (\sigma_p - \sigma_m)/(\sigma_p + 2\sigma_m), & \tau_{MW}\omega << 1 \\ (\varepsilon_p - \varepsilon_m)/(\varepsilon_p + 2\varepsilon_m), & \tau_{MW}\omega >> 1 \end{cases} \quad (12).$$

In addition, in the special case $\varepsilon_m\sigma_p = \varepsilon_p\sigma_m$, the real part of the Clausius-Mossotti function is shown to be frequency independent.

Counterion fluctuation polarisation for DNA

It is the response of the counterions to an externally applied AC electric field that results in counterion polarisation. Since there is Coulombic attraction between the charged body and the counterion layer, the counterions attempt to pull the charged body along with them as they follow the electric field. The counterion polarisation mechanism is due to solution counterions (such as Na^+, Mg^{2+}, etc.) interacting with negatively charged phosphate groups along the DNA or RNA polyion backbone. The counterions move freely along lengths of the biomolecule in response to the component of the external electric field parallel to the major axis or 'backbone', as shown in (Figure 7). Their migration results in an induced dipole moment, and hence, polarisability.

A popular model of counterion polarisation is the 'Mandel-Manning-Oosawa' model developed in various stages by these authors [25-36] and discussed further in [7,37]. In this model, the counterions move freely along biomolecular 'subunit lengths' and are permitted to cross from one subunit to a neighbouring subunit only by overcoming 'potential barriers'. The *subunit*

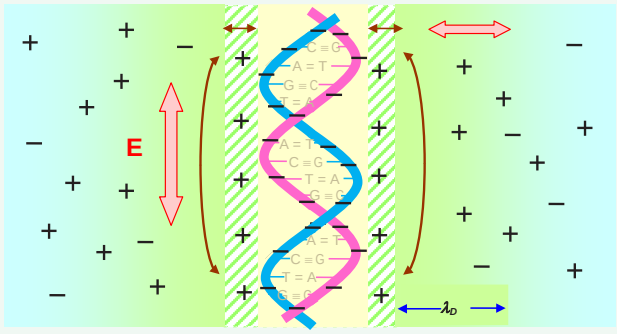

Figure 7 Counterion polarisation on a segment of dsDNA. Counterion polarisation on a short segment of DNA (not to scale): a negatively charged sugar phosphate double helix attracts counterions. Components of an applied AC electric field (red filled bi-directional arrows) causes counterion movement in the longitudinal direction - along the DNA backbone, and transverse direction (brown bi-directional line arrows). The counterion movement tends to be within the 'cylindrical' condensed layer (green shaded /////). The diffuse layer has characteristic length, λ_D, as shown.

length L_s is described as the length along the average biomolecular conformation between 'breaks', or 'potential barriers' resulting from perturbations in the equipotentials (due to conformational processes, folding, etc. Counterions moving along these *subunit* lengths, under the influence of an external electric field, manifest *high* frequency dispersion that is molecular weight *independent*. This polarisation contrasts with *molecular weight dependent* counterion movement along the entire biomolecular contour length that results in *low* frequency dispersion and may account for the static permittivity. A proportion of the counterions are so strongly attracted to the polyelectrolyte that they are said to 'condense' onto the polyion backbone.

Essentially there are three distinct phases:

(i) *Condensed* counterions – these are sufficiently, but non-locally, bound (or 'delocalised') to the phosphate groups of the DNA, and thereby neutralise a fraction of the DNA charge. In many respects the condensed counterion layer is similar to the Stern layer of the double layer model for colloids.

(ii) *Diffuse* counterions which are responsible for neutralising the remainder of the DNA charge, with a density which decreases exponentially with distance from the axis.

(iii) *Bulk* ions or 'added salt' ordinary aqueous solution ions.

In terms of their contribution to polarizability, the condensed counterion phase is the most important. A feature of the condensed state is that the local concentration of counterions around the DNA does not tend to zero when the solvent or bulk electrolyte concentration does. Condensation occurs when the condition $\xi \geq 1/|z|$ is satisfied where z is the valence of each counterion and the charge density parameter, ξ, is given by

$$\xi = q^2 / (4\pi\varepsilon_m k_B T b) \tag{13}$$

where q is the elementary charge, $\varepsilon_m = \varepsilon_0 \varepsilon_{rm}$ is the permittivity of the bulk electrolyte medium, ε_r is the relative permittivity, $k_B T$ is the Boltzmann temperature, and b is the average distance between charged sites; for B-DNA double helix, b = 1.73 Å. The 'Manning-Mandel-Oosawa' model yields a generalised expression for scalar longitudinal polarisability α_s per subunit length L_s,

$$\alpha_s = \frac{z^2 q^2 L_s{}^2 n_{cc} A_{st}}{12 k_B T} \tag{14}$$

where A_{st} is the stability factor of the ionic phase and includes mutual repulsion between fixed charges on the backbone and the effect of Debye screening,

$$A_{st} = [1 - 2(|z|\xi - 1)\ln(\kappa_s b)]^{-1} \tag{15}$$

and the reciprocal of the Debye screening length, shown in (Figure 7), $\lambda_D = \kappa_s^{-1}$ (m) is given by [38],

$$\kappa_s = \left[\left(\frac{N_{Av} q^2}{\varepsilon_m k_B T}\right)\left(\sum_i C_i z^2 + \frac{C_p}{\xi}\right)\right]^{0.5} \tag{16}$$

where N_{Av} is Avogadro's number and C_i and C_p are the respective molar concentrations of ions in the bulk and diffuse phase, and phosphate groups. In the simplifying case where $C_p = 0$, (16) reduces to the standard formula for the Debye reciprocal length of a balanced electrolyte [1,10]. In (14), n_{cc} is the number of condensed counterions that can be predicted theoretically,

$$n_{cc} = \phi_c L_s / (|z| b) \tag{17}$$

where the fraction of condensed counterions is $\phi_c = 1 - |z^{-1}|\xi^{-1}$. Equations (13) to (17) are combined with (4) that determines the polarizability from a dielectric spectroscopy experiment. The relation $\alpha_m C_m = \alpha_S C_S$, where the number density of subunits is $C_S = N_{Av} C_p b / L_S$, ties theory and experiment. An expression for L_s based on the measured dielectric decrement $\Delta\varepsilon'$ is thus derived,

$$L_s = \sqrt{\frac{9\Delta\varepsilon'}{\pi \varepsilon_{rm}(|z|\xi - 1) A_{st} N_{Av} C_p b}} \tag{18}.$$

Assuming, for example, T = 298.2 K (25.0 °C), ε_{rm} = 78.4, z = 1.00 for monovalent cations, C_p = 2.72 mol/m^3 and C_i = 1.10 mol/m^3 then $\xi = 4.132$, $\kappa_S = 9.754 \times 10^7$ (m^{-1}), $A_{st} = 3.764 \times 10^{-2}$ and $L_s = 3.308 \times 10^{-8} \sqrt{\Delta\varepsilon'}$. An expression for the relaxation time in terms of the subunit length was also derived

$$\tau = \frac{L_s{}^2 q}{\pi^2 \mu k_B T} \tag{19}.$$

Assuming the mobility value μ = 8.00×10^{-8} at 25°C temperature, $L_s = 1.424 \times 10^{-4} \sqrt{\tau}$. A sample of dsDNA with measured values, $\Delta\varepsilon'$ = 9 and τ = 500 ns has predicted subunit lengths from (18) and (19) that approximately concur with each other, L_s = 100 nm. Physically, this value is very close to the worm-like chain Kuhn length for dsDNA. In the framework of the counterion model, the result would support the notion that equipotentials arise from natural curvature of the dsDNA suspended in solution. The frequency dependence of the polarizability for 12 kbp dsDNA, for example, [39], was found to correlate with the frequency dependence of the DEP force determined using parameters, e.g. initial DEP collection rates and the initial to steady-state transition [37].

Maxwell-Wagner and other polarization mechanisms for DNA

Interfacial, or *space-charge*, polarisation arises from electrical charges being restricted in their movement at the interfaces between layers of different dielectric materials. Interfacial polarisation results in dielectric dispersions when the aggregate of dissimilar materials is exposed to AC electric fields [1]. Maxwell-Wagner (MW) polarisation models for DNA suspensions have been undertaken by a number of researchers, e.g. [40,41]. A MW interfacial polarisation model considers the DNA biomolecule with the amino acid sugar phosphate double helix as a 2 nm diameter, long cylindrical insulating core with low conductivity and permittivity. The insulator core is surrounded by a highly conducting sheath that represents the bound counterions on the negatively charged sugar phosphate backbone. The conductive sheath interfaces with an electrolyte of low conductivity. Using values for the previous example, the dielectric decrement for MW dispersion for DNA is predicted to give $\Delta\varepsilon' \cong 0.42$, which is very low compared with the counterion model and $f_R \cong 162$ MHz which is comparatively high.

An alternative approach that mimics the rod-shaped DNA biomolecule with conducting sheath by a randomly oriented shelled, prolate ellipsoid with a very short minor axis, and an extremely long major axis also predicted a very high relaxation frequency of hundreds of MHz [35,36]. Since models of MW interfacial polarisation model tend to predict high relaxation frequencies in the order of 100's of MHz, they are less successful model for explaining the dielectric behaviour of DNA than the counterion fluctuation model. This is perhaps because relatively dilute suspensions of DNA exist as worm-like entanglements with a poorly defined interface compared with the well-defined spherical [42], or rod-like boundaries of colloids or some viruses. A variety of other polarisation mechanisms include counterion polarisation transverse to the DNA axis, rotation of water bound molecules along and across the grooves of the DNA, and relaxation of DNA polar groups [12,43-45]. These polarisation mechanisms tend to predict very high frequency dispersions up to hundreds of MHz. Also the relaxation times have temperature dependence that predicts much higher activation energies than measured and tend to have received less significance in the literature [35,36].

DIELECTROPHORESIS

The principles of DEP are often described for an electrically neutral body although in practice the body, such as, DNA is often charged. Application of an electric field external to a neutral body induces an uneven spatial distribution of electrical charge, or *dipoles*, as shown in (Figure 8) where E is the magnitude (peak) of the electric field.

The external electric field also acts on the displaced charges themselves, so that the electric field can be said to act *twice* on the body. If the electric field is uniform, the field flux acting on electrical charges within each localised region yields Coulombic forces that cancel each other and the net force is zero. On the other hand, in a *nonuniform* electric field, Figure 8, the density of the electric flux varies spatially between regions within the body, so that there is an imbalance of Coulombic forces and they sum to a non-zero net force. Assuming the body is more polarisable

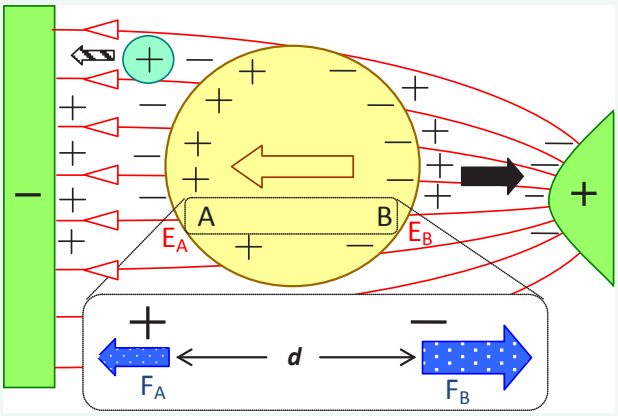

Figure 8 Nonuniform electic field and DEP. Dielectrophoresis: a neutral body (yellow circle) in a nonuniform electric field (red unfilled arrows) experiences a net force depending on the spatial distribution of electric field strength. In this example, where the polarisability of the body is greater than the surrounding medium, it moves to the right (black arrow). A positive test charge (\\\ arrow) moves to the left according to the direction of the electric field flux.

Inset: charges at A and B displaced *d* apart interact with the electric field, E_A and E_B, generating Coulombic forces, F_A and F_B act in opposite directions (blue-filled white-dot patterned arrows), as shown. The force at B is greater than at A, $F_B > F_A$, so the neutral body moves to the right (black filled arrow).

than the surrounding medium, it moves towards the region of highest field non-uniformity (to the right). The imbalance of forces on the neutral body can be modelled by considering two elementary charges $+q$ and $-q$ at A and B, distance d apart, shown in Figure 8 inset. The electric field at B is stronger than at A, $E_B > E_A$. Assuming the forces are acting in the horizontal direction, the sum of the Coulombic forces approximates with a Taylor series,

$$F_{total} = F_A + F_B = qE_B - qE_A = q[E(x+d) - E(x)] \cong q\,d\frac{dE}{dx} \cong p\frac{dE}{dx} \quad (20)$$

where $p = qd$ (C m) is the induced (or effective) dipole moment. This can be written as

$$p = \alpha v E \quad (21)$$

where α is the induced polarisability, or effective dipole moment, per unit volume, v, in unit electric field and has units Farad per metre (Fm^{-1}). It is assumed, for the force to be proportional to the derivative of E in (20), that the length of the dipole p is small compared with the characteristic length of the electric field non-uniformity. Any spatial electric field phase variation is considered to be negligible so that consideration is confined solely to the in-phase component of the DEP force, and that the polarisability is real, $\alpha \in R$. Combining (20) and (21),

$$F_{DEP}\big|_{DC} = \alpha v E\frac{dE}{dx} = \frac{1}{2}\alpha v\frac{dE^2}{dx} \quad (22)$$

where the subscript signifies that this equation is applicable for a constant (DC) signal applied to electrodes and is positive, (i.e. acting towards the right). Expressions for the net force acting on a neutral biomolecule in a nonuniform electric field have also been developed using the energy variation principle and Maxwell stress tensor approach - see discussion [46]. The effective moment method is the most straightforward, and includes situations where there is dielectric loss.

Since the electric field acts twice, *inducing* and *acting on* dipoles within the body, the DEP force predicted by (22) is proportional to the *square* of the magnitude of the electric field. The body moves in accordance with the strength and inhomogeneity of the electric field, the volume and dielectric polarizability of the body, and also the dielectric properties of the suspending medium. Importantly, the net movement of the body does *not* depend on the direction of the electric field or on the electrode polarity. Consequently, time varying alternating current (AC) electrode voltages can be used to move the body rather than constant time Direct Current (DC) potentials. This feature, in turn, avoids problems of hydrolysis reactions occurring between electrode surfaces and bulk medium. AC radio frequencies above a few kHz applied to electrodes in moderately salty electrolytes, for example, do not incur hydrolysis. This enables DEP to be implemented using microelectrodes with micron to sub-micron features for miniaturized applications.

Since AC signals are more useful than DC, the response observable of biomolecules moving in liquids implies that the small-time averaged DEP force is considered. It is evaluated as half the DC value. To accommodate cyclic variations in the electric field, $E = |E|$ is made explicit in (22), the small-time averaged DEP force becomes

$$\begin{aligned} \langle F_{DEP}(x,t)\rangle_T &= \frac{1}{4}\alpha v \frac{d|E|^2}{dx} = \pi r^3 \varepsilon_m \mathrm{Re}\{f_{CM}(\omega)\}\frac{d|E|^2}{dx} \\ &= \pi r^3 \varepsilon_m \frac{d|E|^2}{dx}\left[\frac{(\sigma_p-\sigma_m)(\sigma_p+2\sigma_m)+\omega^2(\varepsilon_p-\varepsilon_m)(\varepsilon_p+2\varepsilon_m)}{(\sigma_p+2\sigma_m)^2+\omega^2(\varepsilon_p+2\varepsilon_m)^2}\right] \end{aligned} \quad (23)$$

where $\langle \ldots \rangle_T$ denotes 'small-time' average over a RF electric field oscillation period, $T = 1/f$. In (23) the second and last terms result from combining (6) and (7) for Maxwell-Wagner polarisation for a sphere with radius, r, and volume, $v = 4\pi r^3/3$.

The expression (23) illustrates three fundamentally important features of DEP. First, if the term in square brackets is positive, $\mathrm{Re}\{f_{CM}(\omega)\} > 0$, then the direction of the force F is governed by $d|E|^2/dx$. Hence, for pDEP, biocolloids (or biomolecules) move *towards* the region of *greatest electric field spatial variation* where $d|E|^2/dx > 0$, typically towards the electrode edges. Conversely, for negative DEP (nDEP) where $\mathrm{Re}\{f_{CM}(\omega)\} < 0$ bio-colloids move *away* from the region of *greatest electric field variation*, typically *away* from the electrode edges. The transition from positive to negative DEP occurs when the DEP force $\vec{F}_{DEP} = 0$ and means that the direction of a DEP driven transport process can be reversed. The *positive-negative* transition may, theoretically, involve any suitable combinations of σ, ε and ω values that force the numerator of (23) to be zero. In practice the parameters controlled in DEP experiments are ω, σ_m, and sometimes ε_m, the other parameters remain constant. Crucially, with today's electronic technology, the RF frequency, ω, can be easily tuned or switched. Consequently, the second feature of (23) is that experimental *cross-over measurements* can be used to find an unknown value for a parameter, e.g. σ_p. Recently, the rate of DEP nanosphere collections has been shown to exhibit excellent repeatability, and have been used as a novel and highly automated way for estimating the value of σ_p [47]. The repeatability also offers new opportunities for temporal response analysis of DEP and related electrokinetic phenomena and the development of real-time image processing methods [48-51].

The third feature of (23) lies in terms of scaling relations used in nanotechnology. A simple and effective way of considering the DEP force is to recall that E is determined by Poisson's or Laplace's equation. This implies (23) shows

$$F_{DEP} \propto \frac{r^3}{d^3}V^2 \quad (24)$$

where d represents the characteristic length of the structure or feature size generating the nonuniform electric field. This means that if r and d decrease by the same amount, i.e. from μm to nm in body and feature size, the DEP force remains the same (subject to the previous caveats). This principle of invariance to scale enables DEP, in principle, to be an attractive means of moving biomolecules on the nanoscale even if earlier work was on the micro-scale or larger. It also remains proportional to the square of the voltage, V, across the electrodes.

Generalizing the first term in (23) to three dimensions,

$$\langle \vec{F}_{DEP}(\underline{x},t)\rangle_T = \vec{F}_{DEP}(\underline{x}) = \frac{1}{4}\alpha(f)v\vec{\nabla}|\vec{E}(\underline{x})|^2 = \frac{1}{2}\alpha(f)v\vec{\nabla}|\vec{E}_{rms}(\underline{x})|^2 \quad (25)$$

where $\vec{\nabla}$ is the gradient operator, '→' denotes vector quantity, the frequency dependence of the polarisability is made explicit, and 'rms' is the root-mean-square. The DEP force is understood to be 'almost instantaneous'. In terms of understanding and computing the DEP force, the electric field gradient for realistic geometric electrode designs can be determined, analytically for simple cases, or by electromagnetic simulation software. The frequency dependent polarizability, α, is inferred from dielectric measurements using (4) or predicted from (7), and the volume is usually known or approximated. For a sphere with radius r with MW polarisation given by (6), the time averaged force given by (25) - with averaging made implicit,

$$\vec{F}_{DEP}(\underline{x}) = 2\pi\varepsilon_m r^3 \mathrm{Re}\{f_{CM}\}\vec{\nabla}\left|\vec{E}_{rms}(\underline{x})\right|^2 \quad (26)$$

and is the starting formula in many scientific publications, e.g. [1,2,7,52].

APPLICATIONS OF DIELECTROPHORESIS TO BIO-MOLECULES

There is much interest in controlling the movement of biomolecules in microfabricated environments for two general application areas. First, for DNA and RNA base sequence and gene expression analyses in LOC and μTAS microdevices and related biotechnological and biomedical applications. Second, using DNA as nano-scaffolds, or constructing material, in molecular electronics. A key motive for this application is that 'top-down' fabrication approaches are limited on the nano-scale so there is strong technological interest in alternative 'bottom-up' approaches. Although there is considerable research on DEP of DNA, there is very little work reported so far on DEP of RNA or PNA. This section starts with an introductory example of quantitative DEP of DNA, and continues on to address wider

contributions from the scientific community to this field.

Dielectrophoresis of DNA: an introductory example

DEP of DNA is typically accomplished with a standard RF signal generator, signal monitoring oscilloscope and measurement apparatus. A wider range of RFs and conductivities can be used but a benchmark RF is 1 MHz with Reverse Osmosis (RO) water or buffer with conductivity less than 1 milliSiemen per metre (mS/m). The measurement process often involves imaging using fluorescence microscopy with modifications that enable recording and data processing. An experimental arrangement for observing DNA transport is shown in (Figure 9(a)). Tracking of DNA biomolecules as they move in real time is achieved by labelling them with a fluorescent dye and observing their micron-scale movement with an epi-fluorescence microscope with typically 200× or above magnification, as shown. Often a camera is used to record and display DNA movement on a PC/TV screen.

A perspective close-up view of the microelectrode interdigitated 'finger' electrodes that are responsible for generating electric fields that drive DEP biomolecule transport is shown in (Figure 9(b)). The thickness of the electrodes, δ_e, has been exaggerated for illustration and is typically, much less than the electrode features, transverse width, w, and interelectrode gap, g, $\delta_e << w, g$. Typical standard microfabricationypical standard microfabrication methods are used: UV patterned resist on glass or other suitable substrate, evaporated with metal, developed, and lift-off. The AC potentials to the electrodes are 180^0 apart so the potential pattern is repeated in the transverse direction every period ($2w+2g$) so the DEP force repeats and is symmetric about each centre of the electrode. The regions of the planar array with the highest nonuniformity are the electrode edges so switching on the DEP attracts the DNA to that region. The DNA is shown to be coiled in the suspension; plasmid DNA for example, has a shape similar to a rubber band that has been, cut, twisted and rejoined again. If the DEP force is sufficiently strong, the coiled DNA collected by the DEP forces becomes stretched by the electric field and builds up to form bridges that span between adjacent electrodes, as shown.

A part video-frame microscope image of DAPI stained 12 kilo-bp (kbp) plasmid DNA, taken from a similar study [37], is shown in (Figure 10(a)) before DEP was applied. The electrodes comprised 10 nm titanium onto glass substrate, 10 nm palladium, overlayed with 100 nm gold with dimensions, $w = g = 10$ μm. The negatively supercoiled plasmid DNA strands cannot be seen individually but they were known to be about 4 μm in contour length or 2 μm looped end-to-end. Figure 10(b) shows the DNA has collected into the interelectrode gap 0.13 s after DEP was applied. One plasmid alone cannot bridge the interelectrode gap, so it is thought that the strands elongate and link to each other, similar to a pearl chain, as they position between the electrodes. The solvent has started to evaporate so the transversally stretched DNA strands have tended to bundle longitudinally in places, as shown. After the DEP force is switched off, Brownian motion is responsible for the DNA strands being released (image not shown) and moving away from the planar array into the bulk solution.

A fluorescence microscope dielectrophoretic spectroscopy

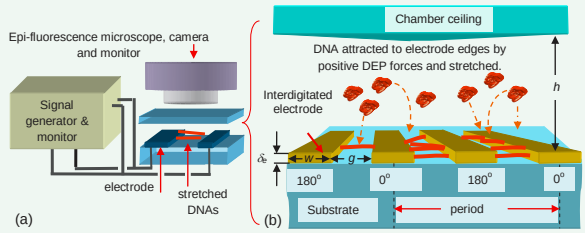

Figure 9 Experimental arrangement for DEP of biomolecules. Scheme of DEP of biomolecule experimental apparatus. (a) AC signal generator, monitoring oscilloscope, epi-fluorescence microscope, camera, monitor, DEP of biomolecule (DNA) collection experiment.

(b) Detailed inset of DEP collection showing interdigitated electrodes (fabricated with features much larger than the thickness δ_e - not to scale) with electrical potential phases 180° apart. DNA molecules are attracted to the interelectrode gaps by positive DEP and stretched, as shown.

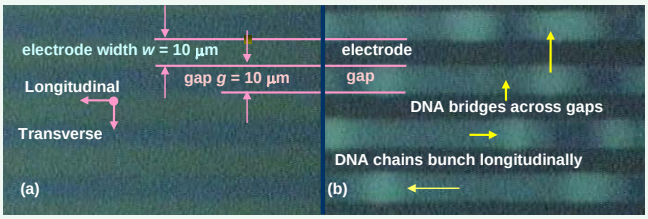

Figure 10 DEP of DNA image (a) DEP off, (b) DEP on. DAPI labeled DNA plasmid suspension: half-frame width images: (a) Before the onset of DEP and (b) 0.13 seconds after the onset of DEP with V_o = 4.5 V, f = 100 kHz.

technique was developed to quantify the DEP collection and release of nanoparticles and DNA [2,37,53]. Since the longitudinal length, l, of the electrodes $l >> w+g$, symmetry and periodicity patterns of the DEP pattern enabled image processing and quantification of video frames comprising a DEP experiment, and resulted in collection and release time profiles. Two quantification summary parameters measured for a designated volume around the electrode, shown in (Figure 9(b)), are (i) the initial collection rate, and (ii) the initial to steady state transition. The former assumes, initially, diffusion is negligible in so that to a first approximation, the amount of fluorescence or DNA collected is proportional to the DEP force over a designated volume. This enabled a comparison of DNA collections and DEP forces for different experimental parameter values, e.g. voltage, frequency dependent polarizability. The later parameter for steady state also allowed comparison for different experimental parameters. The results indicated that the strength of collections also *decreased* with increasing frequency from 100 kHz to 5 MHz, and these trends correlated with dielectric polarizability measurements for the same DNA plasmid [39]. The results also showed that that the predicted DEP force is lower than expected from theory. A number of reasons were presented including the possible effects of AC electroosmosis, polarization saturation, and distortive effect of the DNA on the electric field itself [37].

Dielectrophoresis of DNA

The literature indicates that Washizu's group in Japan pioneered most of the early and novel experiments on DEP of

DNA, starting in the 1990's with their Fluid Integrated Circuit (FIC). The details of their work, [54-64], can be found in several recent and very comprehensive reviews [2,7,52] - along with many important and recent contributions from newly emergent groups around the world. The state-of-the-art and advancement for nanotechnology can be summarised into a couple of general categories.

1. Generation of DEP force, microfabricated environment and DNA preparation

a. The length of DNA that can be moved by DEP depends on the smallest feature size of the electrodes, DNA availability in the volume of solution that can attract DNA, etc., and ranges from 20 bases to tens of kilobases and upwards – limited by the practicalities of sample preparation, e.g. a 1000 kbp or 1 Mega-bp (Mbp) of DNA has a contour length of 340 μm, long enough to be sheared in a micropipette tip during preparation.

i. Many experiments have used 48.5 kbp (contour length 18.5 μm) λ-phage dsDNA, and more recently short sequences (e.g. 20 bp) of ssDNA that are commercially available.

ii. Other types of DNA include 3D DNA origami which entails folded long ssDNA with short (oligonucleotide) ssDNA.

b. Methods for measuring DEP movement:

i. Fluorescence microscopy, as described in the introductory example, has been the standard method for visualising and measuring DEP of DNA. Suitable dyes for visualisation with fluorescence microscopy include DAPI, YOYO, TOTO, acridine orange, PicoGreen.

ii. Other label-free methods include impedance spectroscopy where the presence of the DNA alters the capacitance between the measurement electrodes. An ingenious arrangement is to use the same electrodes for DEP as for measurement and quantification, and was recently reported by Holzel and co-workers [7,65].

c. Voltage and frequency range:

i. Most DEP experiments use standard RF signal generators that range from 0 to 20 MHz and up to 30 volts peak-to-peak. Investigators have tended to use a low frequency range from 30 to 1 kHz or high frequency e.g. 20 kHz to 20 MHz. In principle there are no restrictions except to avoid hydrolysis at low RFs and this, in turn, depends on experimental factors, e.g. solution conductivity. The high frequency response is influenced by impedance characteristics of the electrodes and supply buses.

d. Direct DEP force:

i. 'traditional' DEP uses with metal electrodes that connect directly with buses to the AC supply. The electrodes have often been microfabricated using standard photolithographic methods. Consequently, planar metal electrodes are typically up to a few hundred nanometres in thickness and are essentially quasi-two-dimensional (~2D) with designs that are castellated, triangular, sinusoidal, polynomial, etc., to optimise DEP response. The metals used are gold, aluminium, titanium, platinum, and can be single or multilayered.

ii. Some researchers have also used floating-potential electrodes (FPEs) between the main electrodes in an FIC-type device that do not require connections [59,66].

iii. DEP of DNA, enhanced by nanosized scale of the carbon nanotube (CNT) end features, has been demonstrated where the diameters of the nanotubes were as small as 1 nm. Single- or multi-walled carbon nanotubes (SWCNT or MWCNT) are attractive candidate electrodes since their nanoscale features yield high DEP forces [67-72].

e. Other (indirect) methods for generating a DEP force:

i. Electrode-less DEP (EDEP) or insulating DEP (iDEP) is a powerful method developed less than a decade ago for generating a DEP force by confining an existing uniform electric field using insulating boundaries. The boundaries are made from 3D microfabricated insulating posts made from quartz, polydimethylsiloxane (PDMS), polymethylmethacrylate (PMMA) [73,74] or occurs at the end of a glass nanopipette [75]. Insulating DEP has been recently reviewed [76].

ii. Optically-induced DEP (ODEP) or optoelectronic tweezers (OETs) – as distinguished from 'optical laser tweezers' – have been recently developed where an optical pattern, e.g. from a commercial photo-projector, illuminated onto a photoconductive layer of amorphous silicon, gives rise to a localized DEP force. The optical image has the benefit of acting as an electrode and being able to change position and shape in real-time. It has recently been reported to have manipulated a single DNA biomolecule tethered to a micro-nanosphere [77].

2. DEP of DNA purpose or outcome

a. Electrostatic stretching and trapping of DNA to electrodes using DEP:

i. Temporary positioning: Since DNA is flexible on the micro scale, most reported DEP experiments, in one way or another, involve trapping and positioning DNA for the duration the DEP force is switched on.

ii. Semi-permanent positioning or immobilization: use of chemical modification to bind the DNA to the electrode or substrate so that it remains tethered after the DEP force is switched off, e.g. avidin binding to aluminium (complementary biotin labelling of DNA) and thiol-labelling of gold electrodes (complementary thiol labelling of DNA strands) [78-81] that modified DNA stretching with polymer enhanced media [2,7,52].

iii. Applications of stretching and positioning of DNA include:

- Measuring the lengths of stretched and oriented dsDNA prepared using restriction enzymes and simple cutting of stretched DNA using a UV laser [55,58].
- Measuring the conductivity of DNA for molecular electronics – see the work by Burke [82,83].
- Probing the mechanical elastic properties of DNA [84].
- Molecular surgery: optical tweezer control of a nanosphere coupled to an enzyme, e.g. DNase I, with cutting the bases of electrostatic stretched DNA was demonstrated by [62]. These examples highlight that DNA base information can be used for sub-nanometre position dependent function and underscore the importance of DEP.

- DNA scaffolds: there is a large corpus of literature on DEP of CNTs, metals and their oxides – see [72]. In addition to the current protocols on attachment of metal colloids to DNA, e.g. by Mirkin and co-workers, or in situ growth on substrates, DEP has been proposed for a solution-based method of metallised DNA [85].

b. Separation and purification of DNA:

i. DEP chromatography has been used to separate large (e.g. 48.5 kbp λ-phage dsDNA) and small (22 base ssDNA oligonucleotide) and also medium-large (2 kbp DNA) [63]. Described simply and referring to other descriptions [10,72], the chromatograph is a type of field flow fractionation (FFF) where the DNA solution, driven externally by a pump flow, flows with the fluid lateral to the array (in the transverse direction) left to right and interacts with the vertically DEP-driven force generated by the electrode array. Large DNA biomolecules with strong polarisability and DEP force are pulled down onto the array, whereas small DNA fragments with weak polarisability continue to flow though the chamber, hence, separating the mixture.

ii. The separation of similar sized DNA by DEP has been made possible with nanosphere technology. Called 'DEP enhancement' [63] described the mixing and separation of 35 kbp T7-DNA with 48.5 kbp λ-DNA that had been linked to latex nanospheres. The T7-DNA nanosphere complexes underwent negative DEP whereas the λ-DNA underwent positive DEP, thus, separating the mixture.

c. DEP of DNA has been combined with other biological, chemical and electrokinetic methods, e.g. DC electrophoresis (EP), electroosmosis (EO) and electrostatic liquid actuation. Some recent examples include:

i. Development of DNA concentrators [86]. In that work, the DEP of 26 base ssDNA was compared with low level DC EP (i.e. electrode voltage was sufficiently low, less than a few volts, so that electrolysis did not occur). It was found low level DC EP concentrated the ssDNA better than DEP but the solvent conductivity was low (2 mS/m) and possible degradation to the electrodes by using a DC voltage over time is unclear.

ii. EDEP or iDEP, achieved by using insulating constrictions has resulted in a ten-fold enhancement of DNA hybridization kinetics down to 10 pico-molar concentration sensitivity using relatively high ionic buffer strengths [74].

iii. DEP has also been recently been combined with nanosphere technology to significantly improve the hybridization kinetics of DNA with savings in the use of reagents and with lower ionic strength and simpler protocols than current microarray and Southern blot methods [87]. This offers a molecular scale DEP enhancement and offers promising new advances in detection sensitivity, speed, portability and ease-of-use for genomics research and diagnostics.

iv. DEP has been involved in the lysing of cell contents that include DNA, e.g. from blood samples [88].

d. DEP of DNA in 'packages' or as 'linked':

i. Viruses contain DNA or RNA encapsulated with a protein coat. Viruses have been intensively studied for DEP response, particularly at RFs where the DEP changes from being positive to negative, thus to optimize virus separation [2,7,52].

ii. Chromatin, that constitutes chromosomes and contains DNA wrapped around histones and other proteins, has been lysed from bacteria (*E. coli*) and trapped by DEP at 500 Hz [89].

iii. DNA ligated with PNA and nanospheres showed that DNA could be orientated by DEP unidirectional and moreover imaged using a fluorescence microscope without the need for intercalating dyes [7,65,90].

Dielectrophoresis of RNA

RNA differs chemically from DNA in two important ways. First the pentose sugar ring in DNA, 2' – deoxy-D-ribose, is substituted by D-ribose, as indicated in (Figure 2) Second, one of the bases, Thymine (T), is replaced by Uracil (U) – as also indicated in (Figure 2), so that in RNA, A pairs with U, and C with G.

Basic types of RNA

RNA is mainly involved with reading of DNA, called *transcription*, and its *translation* into proteins and other biomolecules associated with cellular information. There are a number of different types of RNA that perform different functions inside a cell:

(1) Messenger RNA (mRNA) is concerned with transfer of genetic 'blueprint' information that codes for proteins. There are 20 different amino acids (AAs) found in nature, and DNA codes for them using the A, C, G, T base alphabet. This means that it requires a triplet of bases to sufficiently code for 20 AAs. That is, 4 bases to choose independently for first (base) position, 4 bases for the second and so on, yields a total of $4^3 = 64$ possible AAs. This is more than enough to code for the actual 20 AAs needed to make proteins so the genetic code has *redundancy*. The triplet of bases that codes for each AA (and also DNA reading instructions) is called a *codon*.

(2) Transfer RNA (tRNA): reads or decodes each mRNA codon and transfers an appropriate AA onto a polypeptide chain that is being synthesized during production of a particular protein. tRNAs are small RNAs (about 80 nucleotides) with a characteristic clover leaf shape and act as adapters.

(3) Ribosomal RNA (rRNA): ribosomal RNA constitutes part of the ribosome. These are located in the cytoplasm of a cell and are responsible for catalysing the synthesis of AA peptides and hence, protein, by decoding mRNA.

(4) Noncoding RNA is that RNA that is *not* mRNA (does not code for protein) or rRNA or tRNA; and are short ~ 22 nucleotide single strands. These perform a variety of functions that are being currently discovered. These include, for example, small interfering RNA (siRNA) that can silence reading (gene expression) of DNA code, micro RNA (miRNA) that has been linked with cell cycle regulation, cardiac pathology, cancer, etc.

DEP of RNA

There are two challenges facing DEP of RNA research. First, if RNA is extracted, for example, from fish liver cells, the dominant

amount of RNA is rRNA with the other amounts of RNA being much smaller. This means that mRNA needed for understanding protein production, e.g. for gene analysis, has to be carefully separated from the total amount of RNA. Second, RNA tends to be less chemically stable than DNA and precautions are needed to make the laboratory facilities free of degrading enzymes, e.g. RNase.

DEP has been recently used to rapidly collect RNA from the nucleus of a living cancer cell using an Atomic Force Microscope (AFM) [91]. The AFM cone-shaped probe tip had been structurally modified to form nanometer scale concentric electrodes that enabled mRNA to be attracted and subsequently extracted from the cell nucleus. This novel and promising application of DEP may pave the way for enhanced analysis of single cell extracts with many applications, particularly, as the mRNA forms only a small proportion of the total RNA in a cell.

Time dependent DEP collections on of 16S and 23S subunit rRNA, extracted from *E. coli*, onto planar interdigitated over a wide RF range, 3 kHz - 50 MHz, has been recently reported [92]. The in-depth study used an aqueous suspension with conductivity 13 mS/m and revealed positive to negative DEP transition above 9 MHz and a quadratic dependence for low voltages (3Vrms) - as predicted by equations (22) – (26). Being the first demonstration of fast capture and release, DEP shows considerable promise for application in rRNA-based biosensing devices.

Other reports at present have involved DEP of RNA in context, i.e. not as the main focus of study but in conjunction with DEP of DNA, or of cells, e.g. lysing of cell contents [93] or other operations, such as, liquid DEP [94].

OUTLOOK AND CONCLUDING REMARKS

There have been many achievements and DEP of biomolecules, particularly DNA, is an active and promising research field with a scope that has advanced with new materials and technologies e.g. microfluidics, nanospheres, microarrays, nanotubes, electronic nanodevices, and scanning probe microscopes. There is substantial opportunity for advancing theoretical understanding of polarization mechanisms that underpin DEP induced motion of biomolecules in aqueous suspensions; at present, current models favour Maxwell-Wagner polariation for bio-colloidal nanospheres with their well-defined particle-solution interface, and counterion fluctuation for DNA and RNA that form worm-like chains.

There is also considerable opportunity for advancement of laboratory automation methods and nanoscale DEP applications, whether it is directed towards metallization of DNA for nano-construction, or for advancing DNA hybridization kinetics that is needed in genomics and sensor research. DEP of RNA and indeed PNA appears to be research field open for investigation, particularly with the worldwide drive for single cell analysis and quantitative systems biology. There is also much to be accomplished in terms of integrating DEP-based methods with other electrokinetic, LOC and μTAS miniaturization technologies and establishing reliable and quantifiable measures of functionality and performance.

ACKNOWLEDGEMENTS

This work was supported in part by a UCL Enterprise Fellowship (GR/T11364/01) awarded to DH. NV acknowledges the support of an intra-UCL Postdoctoral Mobility Award, which allowed her to spend three fruitful months in the laboratories of Dr David Holmes and Professor Gabriel Aeppli at the London Centre of Nanotechnology. DH would also like to acknowledge the tremendous support and research freedom afforded to him by the late Professor Thomas Duke.

REFERENCES

1. Pohl HA. Dielectrophoresis. Cambridge: Cambridge University Press. 1978.
2. Pethig R. Review article-dielectrophoresis: status of the theory, technology, and applications. Biomicrofluidics. 2010; 4: pii: 022811.
3. Nelson DL, Cox MM, Lehninger Principles of Biochemistry. Fifth ed. New York: Freeman WH. 2008.
4. Pethig R. Dielectric and Electronic Properties of Biological Materials. Chichester: Wiley 1979.
5. Russel WB, Saville DA, Schowalter WR. Colloidal Dispersions. Cambridge, UK: Cambridge University Press.1999.
6. Calladine CR, Drew HR, Luisi BF, Travers AA. Understanding DNA - the molecule and how it works. Third ed. London: Academic Press 2004.
7. Hölzel R. Dielectric and dielectrophoretic properties of DNA. IET Nanobiotechnol. 2009; 3: 28-45.
8. Bloomfield V, Crothers DM, Tinoco JI. Nucleic acids : structures, properties, and functions. Sausalito, Calif.: University Science Books, 2000.
9. Bonincontro A, Giansanti A, Pedone F, Risuleo G. Radiofrequency dielectric spectroscopy of ribosome suspensions. Biochim Biophys Acta. 1991; 1115: 49-53.
10. Morgan H, Green NG. AC electrokinetics. 2003: Research Studies Press, Baldock, England and Institute of Physics Publishing, Philadelphia, USA, 2003.
11. Grant EH, Sheppard RJ, South GP. Dielectric behaviour of biological molecules in solution. Monographs on physical biochemistry, ed. WF Harrington and AR Peacocke. 1978: IoP.
12. Takashima S. Electrical Properties of Biopolymers and Membranes. Bristol: IoP Publishing (Adam Hilger) 1989.
13. O'konski CT. Electric Properties of Macromolecules .V. Theory of Ionic Polarization in Polyelectrolytes. J Phys Chem. 1960; 64: 605-619.
14. Schwarz G. A Theory of Low-Frequency Dielectric Dispersion of Colloidal Particles in Electrolyte Solution. J Phys Chem. 1962; 66: 2636-2642.
15. Schwan HP, Schwarz G, Maczuk J, Pauly H. On Low-Frequency Dielectric Dispersion of Colloidal Particles in Electrolyte Solution1. J Phys Chem. 1962; 66: 2626-2635.
16. Sasaki S, Ishikawa A, Hanai T. Dielectric properties of spherical macroion suspensions. I. Study on monodisperse polystyrene latex. Biophys Chem. 1981; 14: 45-53.
17. Lyklema J, Dukhin SS, Shilov VN. The Relaxation of the Double-Layer around Colloidal Particles and the Low-Frequency Dielectric-Dispersion .1. Theoretical Considerations. J Electroanal Chem. 1983; 143: 1-21.
18. Springer MM, Korteweg A, Lyklema J. The Relaxation of the Double-

Layer around Colloid Particles and the Low-Frequency Dielectric-Dispersion .2. Experiments. J Electroanal Chem. 1983; 153: 55-66.

19. Lyklema J, et al. The Relaxation of the Double-Layer around Colloidal Particles and the Low-Frequency Dielectric-Dispersion .3. Application of Theory to Experiments. J Electroanal Chem. 1986; 198: 19-26.

20. Von Hippel AR. Dielectrics and waves. Artech House, London: John Wiley. 1954.

21. Jones TB. Electromechanics of Particles. Cambridge: Cambridge University Press. 1995.

22. Green NG, Morgan H. Dielectrophoretic investigations of sub-micrometre latex spheres. J Phys D Appl Phys. 1997; 30: 2626-2633.

23. Hughes MP, Morgan H. Dielectrophoretic characterization and separation of antibody coated submicrometer latex spheres. Anal Chem. 1999; 71: 3441-3445.

24. Benguigui L, Lin IJ. More About the Dielectrophoretic Force. J Appl Phys. 1982; 53: 1141-1143.

25. Mandel M. The Electric Polarization of Rod-Like, Charged Macromolecules. Mol Phys. 1961; 4: 489-496.

26. Van der Touw F, Mandel M. Dielectric Increment and Dielectric-Dispersion of Solutions Containing Simple Charged Linear Macromolecules .1. Theory. Biophysical Chemistry. 1974; 2: 218-230.

27. Van der Touw F, Mandel M. Dielectric Increment and Dielectric-Dispersion of Solutions Containing Simple Charged Linear Macromolecules .2. Experimental Results with Synthetic Polyelectrolytes. Biophysical Chemistry. 1974; 2: 231-241.

28. Vreugdenhil T, van der Touw F, Mandel M. Electric permittivity and dielectric dispersion of low-molecular weight DNA at low ionic strength. Biophys Chem. 1979; 10: 67-80.

29. Mandel M, Odijk T. Dielectric-Properties of Poly-Electrolyte Solutions. Annu Rev Phys Chem 1984; 35: 75-108.

30. Manning GS. Limiting Laws and Counterion Condensation in Polyelectrolyte Solutions .I. Colligative Properties. J Chem Phys. 1969; 51: 924.

31. Manning GS. The molecular theory of polyelectrolyte solutions with applications to the electrostatic properties of polynucleotides. Q Rev Biophys. 1978; 11: 179-246.

32. Manning GS. Limiting laws and counterion condensation in polyelectrolyte solutions. V. Further development of the chemical model. Biophys Chem. 1978; 9: 65-70.

33. Oosawa F. Counterion Fluctuation and Dielectric Dispersion in Linear Polyelectrolytes. Biopolymers. 1970; 9: 677.

34. Oosawa F. Polyelectrolytes. New York, USA: Marcel Dekker. 1971.

35. Bone S, Small CA. Dielectric studies of ion fluctuation and chain bending in native DNA. Biochim Biophys Acta. 1995; 1260: 85-93.

36. Bone S, Lee RS, Hodgson CE. Dielectric studies of intermolecular interactions in native DNA. Biochim Biophys Acta. 1996; 1306: 93-97.

37. Bakewell DJ, Morgan H. Dielectrophoresis of DNA: Time- and frequency-dependent collections on microelectrodes. IEEE Transactions on Nanobioscience. 2006; 5: 139-146.

38. Penafiel LM, Litovitz TA. High-Frequency Dielectric-Dispersion of Polyelectrolyte Solutions and Its Relation to Counterion Condensation. J Chem Phys. 1992; 97: 559-567.

39. Bakewell DJ, Ermolina I, Morgan H, Milner J, Feldman Y. Dielectric relaxation measurements of 12 kbp plasmid DNA. Biochim Biophys Acta. 2000; 1493: 151-158.

40. Grosse C. Microwave-Absorption of Suspensions of DNA Type Particles in Electrolyte Solution. Alta Frequenza. 1989; 58: 365-368.

41. Saif B, Mohr RK, Montrose CJ, Litovitz TA. On the mechanism of dielectric relaxation in aqueous DNA solutions. Biopolymers. 1991; 31: 1171-1180.

42. Bonincontro A, Cametti C, Di Biasio A, Pedone F. Effect of ions on counterion fluctuation in low-molecular weight DNA dielectric dispersions. Biophys J. 1984; 45: 495-501.

43. de Xammar Oro JR, Grigera JR. Dielectric properties of aqueous solutions of sonicated DNA above 40 MHz. Biopolymers. 1984; 23: 1457-1463.

44. Satoru Mashimo, Toshihiro Umehara, Shinichi Kuwabara, Shin Yagihara. Dielectric Study on Dynamics and Structure of Water Bound to DNA Using a Frequency-Range 107-1010 Hz. J Phys Chem. 1989; 93: 4963-4967.

45. Umehara T, Kuwabara S, Mashimo S, Yagihara S. Dielectric study on hydration of B-, A-, and Z-DNA. Biopolymers. 1990; 30: 649-656.

46. Wang XJ, Wang XB, Gascoyne PRC. General expressions for dielectrophoretic force and electrorotational torque derived using the Maxwell stress tensor method. J Electrostat. 1997; 39: 277-295.

47. Bakewell DJ, Holmes D. Dual-cycle dielectrophoretic collection rates for probing the dielectric properties of nanoparticles. Electrophoresis. 2013; 34: 987-999.

48. Bakewell DJ. Modelling nanoparticle transport in dielectrophoretic microdevices using a Fourier-Bessel series and applications for data analysis. J Phys D Appl Phys. 2011; 44: 1-16.

49. Bakewell DJ, Chichenkov A. Fourier-bessel series modeling of dielectrophoretic bionanoparticle transport: principles and applications. IEEE Trans Nanobioscience. 2012; 11: 79-86.

50. Bakewell DJ, Chichenkov A. Quantifying dielectrophoretic nanoparticle response to amplitude modulated input signal. J Phys D Appl Phys. 2012; 45:1-15.

51. Bakewell DJ, Chichenkov A. Quantifying dielectrophoretic nanoparticle response to amplitude modulated input signal (vol 45, 365402, 2012). J Phys D Appl Phys. 2012; 45(49):1-2.

52. Lapizco-Encinas BH, Rito-Palomares M. Dielectrophoresis for the manipulation of nanobioparticles. Electrophoresis. 2007; 28: 4521-4538.

53. Bakewell DJ, Morgan H. Quantifying dielectrophoretic collections of sub-micron particles on microelectrodes. Meas Sci Technol. 2004; 15: 254-266.

54. Washizu M. Electrostatic Manipulation of Biological Objects. J Electrostat. 1990; 25: 109-123.

55. Washizu M, Kurosawa O. Electrostatic Manipulation of DNA in Microfabricated Structures. IEEE Transactions on Industry Applications. 1990; 26: 1165-1172.

56. Washizu M, Shikida M, Aizawa S, Hotani H. Orientation and Transformation of Flagella in Electrostatic-Field. IEEE Transactions on Industry Applications. 1992; 28: 1194-1202.

57. Washizu M, Suzuki S, Kurosawa O, Nishizaka Takeshi, Shinohara. Molecular dielectrophoresis of biopolymers. IEEE Transactions on Industry Applications. 1994; 30: 835-843.

58. Washizu M, Kurosawa O, Arai Ichiro, Suzuki S, Shimamoto N. Applications of Electrostatic Stretch-and-Positioning of DNA. IEEE Transactions on Industry Applications.1995; 31: 447-456.

59. Washizu M. Biological applications of electrostatic surface field effects. J Electrostat. 2005. 63: 795-802.

60. Kabata H, Kurosawa O, Arai I, Washizu M, Margarson SA, Glass RE, et al. Visualization of single molecules of RNA polymerase sliding along DNA. Science. 1993; 262: 1561-1563.

61. Kabata HW, Okada W, Washizu M. Single-molecule dynamics of the Eco RI enzyme using stretched DNA: its application to in situ sliding assay and optical DNA mapping. Jpn J Appl Phys. 2000; 39: 7164-7171.

62. Yamamoto T, Kurosawa O, Kabata H, Shimamoto N, Washizu M. Molecular surgery of DNA based on electrostatic micromanipulation. IEEE Trans Ind Appl. 2000; 36: 1010-1017.

63. Kawabata T, Washizu M. Dielectrophoretic detection of molecular bindings. IEEE Trans Ind Appl. 2001; 37: 1625-1633.

64. Kurosawa O, Washizu M. Dissection, acquisition and amplification of targeted position of electrostatically stretched DNA. J Electrostat.2007; 65: 423-430.

65. Henning A, Bier FF, Hölzel R. Dielectrophoresis of DNA: Quantification by impedance measurements. Biomicrofluidics. 2010; 4.

66. Asbury CL, van den Engh G. Trapping of DNA in nonuniform oscillating electric fields. Biophys J. 1998; 74: 1024-1030.

67. Tuukkanen S, Toppari JJ, Hytonen VP, Kuzyk A, Kulomaa MS, Torma P. Dielectrophoresis as a tool for nanoscale DNA manipulation. Int J Nanotechnol. 2005. 2: 280-291.

68. Tuukkanen S, Kuzyk A, Toppari JJ, Hytönen VP, Ihalainen T, Törmä1 P. Dielectrophoresis of nanoscale double-stranded DNA and humidity effects on its electrical conductivity. Appl Phys Lett. 2005; 87.

69. Tuukkanen S, Toppari JJ, Kuzyk A, Hirviniemi L, Hytönen VP, Ihalainen T, et al. Carbon nanotubes as electrodes for dielectrophoresis of DNA. Nano Lett. 2006; 6: 1339-1343.

70. Sampo Tuukkanen, Anton Kuzyk, Jussi Toppari J, Hannu Hakkinen, Vesa P Hytonen, Einari Niskanen, et al. Trapping of 27 bp-8 kbp DNA and immobilization of thiol-modified DNA using dielectrophoresis. Nanotechnology. 2007; 18.

71. Regtmeier J, Eichhorn R, Bogunovic L, Ros A, Anselmetti D. Dielectrophoretic trapping and polarizability of DNA: the role of spatial conformation. Anal Chem. 2010; 82: 7141-7149.

72. Zhang C, Khoshmanesh K, Mitchell A, Kalantar-Zadeh K. Dielectrophoresis for manipulation of micro/nano particles in microfluidic systems. Anal Bioanal Chem. 2010; 396: 401-420.

73. Chou CF, Tegenfeldt JO, Bakajin O, Chan SS, Cox EC, Darnton N, et al. Electrodeless dielectrophoresis of single- and double-stranded DNA. Biophys J. 2002; 83: 2170-2179.

74. Swami N, Chou CF, Ramamurthy V, Chaurey V. Enhancing DNA hybridization kinetics through constriction-based dielectrophoresis. Lab Chip. 2009; 9: 3212-3220.

75. Ying L, White SS, Bruckbauer A, Meadows L, Korchev YE, Klenerman D. Frequency and voltage dependence of the dielectrophoretic trapping of short lengths of DNA and dCTP in a nanopipette. Biophys J. 2004; 86: 1018-1027.

76. Regtmeier J, Eichhorn R, Viefhues M, Bogunovic L, Anselmetti D. Electrodeless dielectrophoresis for bioanalysis: theory, devices and applications. Electrophoresis. 2011; 32: 2253-2273.

77. Lin YH, Chang CM, Lee GB. Manipulation of single DNA molecules by using optically projected images. Opt Express. 2009; 17: 15318-15329.

78. Germishuizen WA, Walti C, Wirtz R, Johnston MB, Pepper M, Davies AG, et al. Selective dielectrophoretic manipulation of surface-immobilized DNA molecules. Nanotechnology. 2003; 14: 896-902.

79. Germishuizen WA, Tosch P, Middelberg APJ, Wälti C, Davies AG, Wirtz R, et al. Influence of alternating current electrokinetic forces and torque on the elongation of immobilized DNA. J Appl Phys. 2005; 97.

80. Sung KE, Burns MA. Optimization of dielectrophoretic DNA stretching in microfabricated devices. Anal Chem. 2006; 78: 2939-2947.

81. Lin R, Burke DT, Burns MA. Selective extraction of size-fractioned DNA samples in microfabricated electrophoresis devices. J Chromatogr A. 2003; 1010: 255-268.

82. Zheng L, Li S, Brody JP, Burke PJ. Manipulating nanoparticles in solution with electrically contacted nanotubes using dielectrophoresis. Langmuir. 2004; 20: 8612-8619.

83. Zheng L, Brody JP, Burke PJ. Electronic manipulation of DNA, proteins, and nanoparticles for potential circuit assembly. Biosens Bioelectron. 2004; 20: 606-619.

84. Dalir H, Yanagida Y, Hatsuzawa T. Probing DNA mechanical characteristics by dielectrophoresis. Sens Actuators B Chem. 2009; 136: 472-478.

85. Swami AS, Brun N, Langevin D. Phase Transfer of Gold Metallized DNA. Journal of Cluster Science. 2009; 20: 281-290.

86. Yokokawa R, Manta Y, Namura M, Takizawa Y, Le Nam CH, Sugiyama S. Individual evaluation of DEP, EP and AC-EOF effects on lambda DNA molecules in a DNA concentrator. Sens Actuators B Chem. 2010; 143: 769-775.

87. Cheng IF, Senapati S, Cheng X, Basuray S, Chang HC, Chang HC. A rapid field-use assay for mismatch number and location of hybridized DNAs. Lab Chip. 2010; 10: 828-831.

88. Sonnenberg A, Marciniak JY, McCanna J, Krishnan R, Rassenti L, Kipps TJ, et al. Dielectrophoretic isolation and detection of cfc-DNA nanoparticulate biomarkers and virus from blood. Electrophoresis. 2013; 34: 1076-1084.

89. Prinz C, Tegenfeldt JO, Austin RH, Cox EC, Sturm JC. Bacterial chromosome extraction and isolation. Lab Chip. 2002; 2: 207-212.

90. Du ML, Bier FF, Hölzel R. Quantifying DNA dielectrophoresis. AIP Conf Proc. 2006; 859: 65-72.

91. Nawarathna D, Chang R, Nelson E, Wickramasinghe HK. Targeted messenger RNA profiling of transfected breast cancer gene in a living cell. Anal Biochem. 2011; 408: 342-344.

92. Giraud G, Pethig R, Schulze H, Henihan G, Terry JG, Menachery A, et al. Dielectrophoretic manipulation of ribosomal RNA. Biomicrofluidics. 2011; 5: 24116.

93. Cheng J, Sheldon EL, Wu L, Uribe A, Gerrue LO, Carrino J, et al. Preparation and hybridization analysis of DNA/RNA from E. coli on microfabricated bioelectronic chips. Nat Biotechnol. 1998; 16: 541-546.

94. Collard D, Kim SH, Osaki T, Kumemura M, Kim B, Fourmy D, et al. Nano bioresearch approach by microtechnology. Drug Discov Today. 2013; 18: 552-559.

Cite this article

Bakewell DJ, Vergara-Irigaray N, Holmes D (2013) Dielectrophoresis of Biomolecules. JSM Nanotechnol Nanomed 1(1): 1003.